Dynamic Identification of a Mitsubishi PA10-6CE Robot using Motion Capture

Chris Lightcap and Scott Banks

Abstract—**This paper discusses a method to identify dynamic parameters in a rigid-link flexible-joint robot model using motion capture. The procedure is divided into two parts. First, the robot dynamics are parameterized in a new form to exclude the stiffness torque, and are solved with a rich set of data. The stiffness torque is then reconstructed from the new parameter set, and a torsional spring model is fit to the measured data. This method offers a better conditioned system of equations for weakly-flexible systems, and more flexibility in the choice of torsional spring model. The two-step identification method is experimentally evaluated on a Mitsubishi PA10-6CE.**

I. INTRODUCTION

It has been shown that improved tracking performance is possible with an accurate dynamic robot model. Precise and reliable identification methods are well documented for rigid-link rigid-joint robots. However, relatively flexible harmonic drives are being used more frequently in lightweight, high performance robots. The Mitsubishi PA10-6CE is assembled with such a transmission and is known to deflect under load. Identification must account for these effects in order to develop an accurate physical model. Yet methods for robot manipulators with flexible joints are still in development.

Typically, parameter identification of robot manipulators is performed in the frequency-domain or time-domain. Frequency-domain identification methods reduce the robot dynamics to a pair of second order linear differential equations under the small angle assumption. Parameters are identified through nonlinear optimization with a cost function defined as the sum of the squared differences between predicted and measured outputs of the system at different frequencies [1]. Design variables can be chosen as the polynomial coefficients which define the system transfer function or the physical parameters of the robot.

Li et al. reported a frequency domain technique that combined the finite element method with experimental modal analysis to identify stiffness and damping coefficients [2]. Link dynamics were excited with mechanical impulses and the responses were compared to an analytic model to determine robot parameters. The objective function was defined as the sum of the squared error between the natural frequencies obtained from the analytical model and those obtained from the experiment. Frequency-domain methods provide good estimates for parameters in a linear model but fail to identify nonlinearities, such as mass center and coulomb friction parameters.

Alternatively, the dynamic model of the robot can be obtained through direct experimentation. Taghirad et al. developed a model of harmonic drive stiffness through a controlled loading experiment of a one-link manipulator [3]. Albu-Schaffer et al. proposed the identification of joint flexibilities prior to assembly [4]. They derived a linearized form of the flexible-joint dynamics under the small angle assumption and satisfied this condition by fixing the motor position with an electro-magnetic brake. They excited the link dynamics with mechanical impulses and measured the response of the system. Nonlinear optimization was used to determine flexibility and damping parameters from the impulse response.

Identification in the time-domain is most often performed with linear least-squares methods. A solution is achieved through linear parameterization of the robot dynamics into a regressor matrix, containing functions of the known joint displacement, and an array of unknown parameters [5]. An over-determined system of equations is formed with sampled data and solved with least-squares techniques.

Desired trajectories for identification can be determined by selecting appropriate optimization criteria. Researchers often minimize the condition number of the regressor matrix, or maximize its minimum singular value, thus improving the robustness of the numerical solution to measurement noise [6]. Calafiore et al. minimized the covariance matrix of parameter estimates by maximizing the Fisher information matrix [7]. The design variables in both cases are the Fourier coefficients or polynomial coefficients defining the proposed robot trajectory.

Pham et al. proposed a linear parameterization of the flexible-joint dynamics and explained two methods for parameter identification [8]. The first method requires augmenting the sensing capabilities of the robot with additional joint encoders. The latter identification method compensates for unmeasurable link position, but the link masses and coulomb friction parameters are lost. Pham et al. did not discuss trajectory optimization for improved parameter estimation.

This paper discusses a method for dynamic parameter identification of a rigid-link flexible joint robot using motion capture. Section II discusses the reformulated parameterization of the robot dynamics and subsequent trajectory optimization. Section III details our method for estimation of link position using motion capture. Section IV discusses an experimental procedure for the Mitsubishi PA10-6CE robot.

Manuscript received April 9, 2007. This work was supported by new faculty startup funds at the University of Florida.

C. Lightcap is with the Department of Mechanical and Aerospace Engineering, University of Florida, Gainesville, FL 32611 USA (phone: 352-392-9638; fax: 352-392-9638; e-mail: cal9@ufl.edu).

S. Banks is with the Department of Mechanical and Aerospace Engineering and the Department of Orthopaedics and Rehabilitation, University of Florida, Gainesville, FL 32611 USA (e-mail: banks@ufl.edu).

Sections V and VI provide experimental results and conclusions.

II. Rigid-Link Flexible-Joint Model

The n-link rigid-link flexible-joint (RLFJ) robot dynamics can be expressed as [9]

$$\begin{aligned} M(q)\ddot{q} + V_m(q,\dot{q})\dot{q} + G(q) + F(\dot{q}) + K(q - q_m) &= 0 \\ J\ddot{q}_m + B\dot{q}_m + K(q_m - q) &= u, \end{aligned} \tag{1}$$

where $q(t), \dot{q}(t), \ddot{q}(t) \in \Re^n$ and $q_m(t), \dot{q}_m(t), \ddot{q}_m(t) \in \Re^n$ denote the position, velocity, and acceleration of the link and motor angle, respectively, $M(q) \in \Re^{n \times n}$ represents the positive-definite inertia matrix, $V_m(q,\dot{q}) \in \Re^{n \times n}$ represents the centripetal-Coriolis matrix, $G(q) \in \Re^n$ and $F(\dot{q}) \in \Re^n$ denote the gravitational and frictional effects of the link dynamics, respectively, $K, J, B \in \Re^n$ are constant, diagonal, positive-definite matrices representing joint stiffness, motor inertia, and motor viscous friction, respectively, and $u(t) \in \Re^n$ denotes the motor torque.

Accordingly, the one-link RLFJ robot dynamics can be written as

$$\begin{aligned} I\ddot{q} - mgl_x \sin(q) + mgl_y \cos(q) + c\, sign(\dot{q}) + v\dot{q} + k(q - q_m) &= 0 \\ J\ddot{q}_m + b\dot{q}_m + k(q_m - q) &= u, \end{aligned} \tag{2}$$

where $q(t), \dot{q}(t), \ddot{q}(t) \in \Re$ and $q_m(t), \dot{q}_m(t), \ddot{q}_m(t) \in \Re$ denote the position, velocity, and acceleration of the link and motor angles, respectively, and $I, m, c, v, k, J, b \in \Re$ are the unknown parameters representing link inertia, link mass, coulomb and viscous friction, joint stiffness, motor inertia, and motor viscous friction, respectively.

A. Least-Squares Parameter Identification

The one-link RLFJ robot dynamics, given by (2), can be linear parameterized as the following expression:

$$\begin{bmatrix} \ddot{q} & -\sin(q) & \cos(q) & sign(\dot{q}) & \dot{q} & q - q_m & 0 & 0 \\ 0 & 0 & 0 & 0 & 0 & q_m - q & \ddot{q}_m & \dot{q}_m \end{bmatrix} \begin{bmatrix} I \\ mgl_x \\ mgl_y \\ c \\ v \\ k \\ J \\ b \end{bmatrix} = \begin{bmatrix} 0 \\ u \end{bmatrix} \tag{3}$$

To identify elements in the regressor matrix, motor positions, link positions, and motor torques are recorded as the link follows a desired trajectory. The unknown model parameters are then determined by forming an overdetermined system of equations from the measured data. The problem can be simplified into the following expression and solved with least-squares methods.

$$\begin{aligned} &Y(q, \dot{q}, \ddot{q}, q_m, \dot{q}_m, \ddot{q}_m)\theta = x, \\ &\text{where } \theta = \left(Y^T Y\right)^{-1} Y^T x. \end{aligned} \tag{4}$$

The moment of inertia obtained from a single-joint experiment is a composite of all links between the end-effector and the moving joint. Individual link inertias can be obtained in a sequential manner using the parallel axis theorem and group inertia properties.

The formulation of the system of equations in (4) is problematic for a robot with weak joint elasticity. In this scenario, the joint deflections are small compared to the link and motor kinematics, resulting in a poorly-scaled and ill-conditioned matrix. The condition number can be reduced by rewriting the one-link dynamics to eliminate the stiffness term as follows:

$$\begin{aligned} I\ddot{q} - mgl_x \sin(q) + mgl_y \cos(q) + c\, sign(\dot{q}) + v\dot{q} \\ + J\ddot{q}_m + b\dot{q}_m = u. \end{aligned} \tag{5}$$

The dynamics are then parameterized as

$$\begin{bmatrix} \ddot{q} & -\sin(q) & \cos(q) & sign(\dot{q}) & \dot{q} & \ddot{q}_m & \dot{q}_m \end{bmatrix} \begin{bmatrix} I \\ mgl_x \\ mgl_y \\ c \\ v \\ J \\ b \end{bmatrix} = u \tag{6}$$

The formulation in (6) is better posed for a robot with weak joint elasticity. The omission of joint deflection from the regressor matrix eliminates the scaling problem. Joint stiffnesses are determined subsequent to the identification of inertial and frictional model parameters. The stiffness torque, or torque transmitted through the torsional spring, is determined from the following expression.

$$\begin{aligned} \tau_s &= I\ddot{q} - mgl_x \sin(q) + mgl_y \cos(q) + c\, sign(\dot{q}) + v\dot{q} \\ &= K(q_m - q) \end{aligned} \tag{7}$$

A suitable stiffness model can be selected by examining the relationship between joint deflection and stiffness torque obtained in (7).

B. Trajectory Optimization

In the dynamic identification of rigid-link rigid-joint (RLRJ) manipulators, the desired link trajectory is carefully selected to sufficiently excite all dynamics. The optimization criteria are commonly chosen as the condition number of the regressor matrix or the determinant of the Fisher information matrix. The case of RLFJ robot dynamics is no different. An optimal excitation trajectory can be determined from the

constrained nonlinear optimization:

$$\min cond(Y(q,\dot{q},\ddot{q},\dot{q}_m,\ddot{q}_m)) \quad s.t. \quad \begin{cases} q_{\min} < q_m(t) < q_{\max} \\ -\dot{q}_{\max} < \dot{q}_m(t) < \dot{q}_{\max} \end{cases}, \tag{8}$$

where the regressor matrix is now a function of both the motor position and link position. The excitation trajectory, or motor position, can be parameterized as a finite Fourier series [6].

$$q_m(t) = q_o + \sum_{n=1}^{N} \frac{a_n}{n\omega_f}\sin(n\omega_f t) - \frac{b_n}{n\omega_f}\cos(n\omega_f t) \tag{9}$$

The design variables are the amplitudes of the fundamental frequency and *N*-1 harmonics. The fundamental frequency should be chosen near the natural frequency of the system if the motor command cycle and joint position sampling frequencies will permit.

In the case of RLFJ robot dynamics, the regressor matrix is a function of both motor position and link position. However, link position cannot be parameterized independent of motor position because it is a function of the robot dynamics. It should be determined with an approximation of the robot model and forward dynamics. The link acceleration can be estimated from

$$\ddot{q} = I^{-1}\left(mgl_x \sin(q) - mgl_y \cos(q) - c\,sign(\dot{q}) - v\dot{q} - k(q - q_m)\right), \tag{10}$$

and, given the initial state of the robot, can be integrated to obtain link positions and velocities.

An exciting trajectory determined for link 2 of the Mitsubishi PA10-6CE robot is shown in Fig. 1.

III. Estimation of Link Position

Typical robotic systems are assembled with one joint resolver or encoder for each link, and therefore have insufficient sensing hardware for a RLFJ model. To overcome this limitation, motion capture markers are fixed to the external surface of the robot to provide an estimate of the link position (Fig. 2).

The axis of rotation and respective center of rotation for each link can be determined from a sufficiently rich set of marker data. The analytic solution for an axis of rotation obtained in [10] minimizes the cost function

$$E = \sum_{p=1}^{P}\sum_{k=1}^{N}\left[\left(\vec{v}_k^{\,p} - \vec{m}^{\,p}\right)\cdot\vec{n}\right], \tag{11}$$

where $\vec{n}$ is a unit vector in the direction of the axis of rotation, $\vec{v}_k^{\,p}$ is the observed position of marker *p* in frame *k*, and $\vec{m}^{\,p}$ is the center of rotation of marker *p*. An unbiased least-squares solution for a point on the axis of rotation is obtained in [11] given the cost function

$$E = \sum_{p=1}^{P}\sum_{k=1}^{N}\left[\left(\vec{v}_k^{\,p} - \vec{m}\right)^2 - \left(r^{\,p}\right)^2\right]^2, \tag{12}$$

where $\vec{m}$ is any point on the axis of rotation, and $r^{\,p}$ is the radius of the circle mapped out by marker *p*.

After the position of each marker relative to its neighboring axis of rotation is known, link position is determined through nonlinear optimization [12]. The cost function is defined as

$$E = \min_{q}\sum_{p=1}^{P}\left(\vec{v}_k^{\,p} - \hat{\vec{v}}_k^{\,p}(q)\right)^2, \tag{13}$$

where $\vec{v}_k^{\,p}$ is the measured position of marker *p* in frame *k*, and $\hat{\vec{v}}_k^{\,p}(q)$ is the predicted marker position given an angle of rotation *q*. The initial guess for the first frame is selected as the initial motor position. Subsequent frames are seeded with the preceding link position.

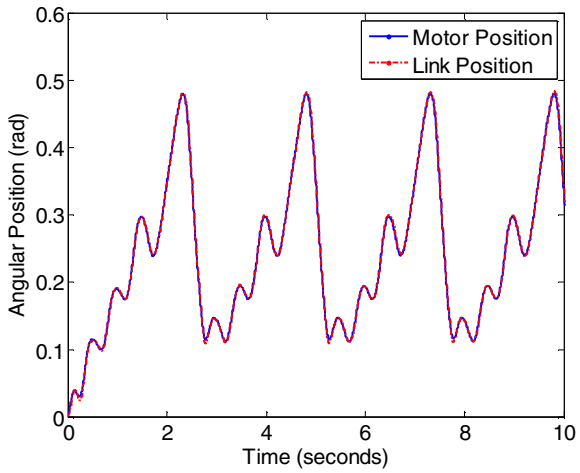

Fig. 1 Identification Trajectory for Link 2.

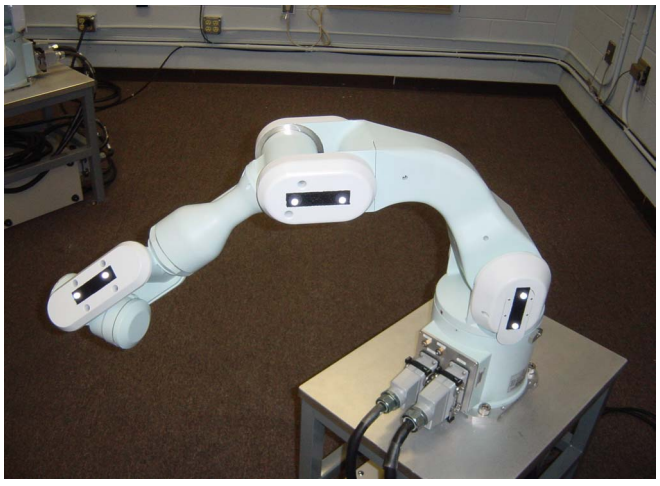

Fig. 2 Motion Capture Markers on PA10-6CE.

IV. Experimental Methods

A. Experimental Setup

A Mitsubishi PA10-6CE robot was mounted on a steel frame table with a height of 0.6 m. The table was attached to the floor with a set of four bolts and internally-threaded concrete anchors. The robot was positioned in the center of the viewing volume of an eight-camera passive-marker motion camera system (Motion Analysis Corporation, Santa Rosa, CA). The residual measurement error obtained through calibration was on the order of 0.3 mm, with a standard deviation of 0.1 mm. Clusters of three or four reflective markers were positioned on the exterior surface of four links. Real-time measurement and control of the robot and motion capture system was achieved with a Linux kernel patched with *RTAI-LXRT*, and the *OROCOS* and *ORCA* software libraries [13], [14].

An end-effector apparatus was designed and constructed to support additional load on the robot end-effector (Fig. 3). A 44.5 N load was attached to the device to excite robot inertial and stiffness dynamics. A description of each link coordinate system is included in Fig. 4.

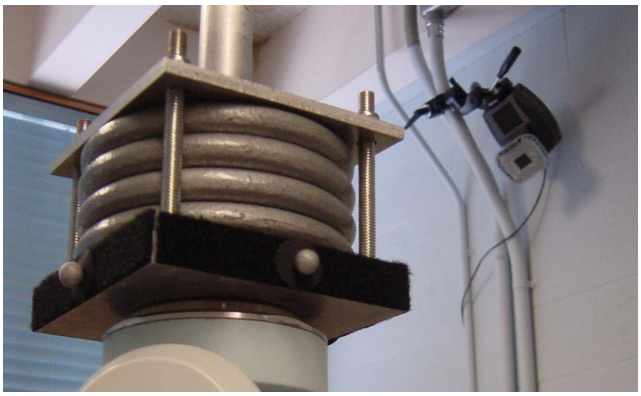

Fig. 3 End-Effector Weight Rack

B. Identification of Mass, Inertia, and Friction

The robot was commanded to follow, for each joint, the single-joint trajectory obtained from minimization of the regressor matrix condition number. The remaining links were fixed with electro-magnetic brakes. Motor position was recorded with joint resolvers, with a reported ±10 arc min electric error and ±22 arc min R/D converter error [15], leading to an overall accuracy of ±0.64 arc min (0.011 deg) for the angular position of the motor (gear ratio = 50). Motor torque was determined from the input current and the motor constant. Link position was estimated from the measurement of motion capture markers on the surface of the robot. The sampling frequency of the motion capture system was 250 Hz. Least-squares and nonlinear optimization algorithms were performed in MATLAB (Mathworks, Natick, MA).

The experiment was repeated 10x for each link. The coefficient of variation (CV) of an estimated parameter, a measure of its fidelity, was defined as the ratio of the standard deviation to the sample mean of the population. The sample mean of each parameter and its CV were recorded for each experiment.

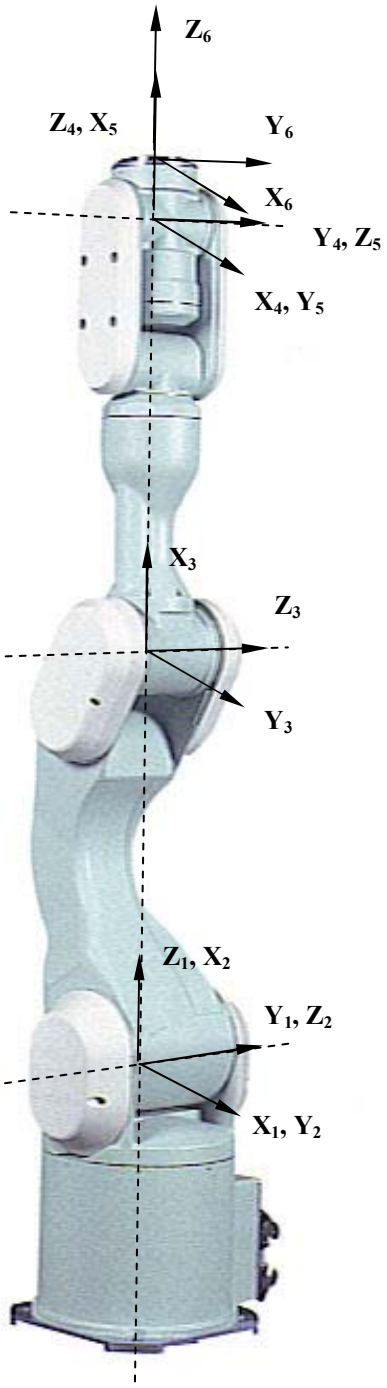

Fig. 4 Coordinate System Definitions

C. Identification of Joint Stiffness

Linear stiffness coefficients were determined for each experiment after the identification of inertial, mass center, and frictional parameters. The correlation coefficient r^2 was also determined for each experiment.

V. Experimental Results

A. Estimation of Link Position

The root-mean-square (RMS) error in the estimation of marker radius r^p was not greater than 0.3 mm for all measured trials. The RMS error in reconstructed marker position from joint angle optimization was between 0.5 and 1.1 mm for all measured trials.

B. Least-Squares Parameter Identification

Model parameters and their coefficients of variation are reported in Table I. The coulomb friction parameters were equal to [9.08, 9.28, 5.81, 1.48, 1.84, 0.87] Nm for joints 1 through 6, respectively. Mean RMS errors between measured and reconstructed torques were equal to [2.48, 19.33, 6.55, 0.56, 1.37, 0.33] Nm, for joints 1 though 6, respectively. A plot of the measured torque and predicted torque for joint 2 is shown in Fig. 5.

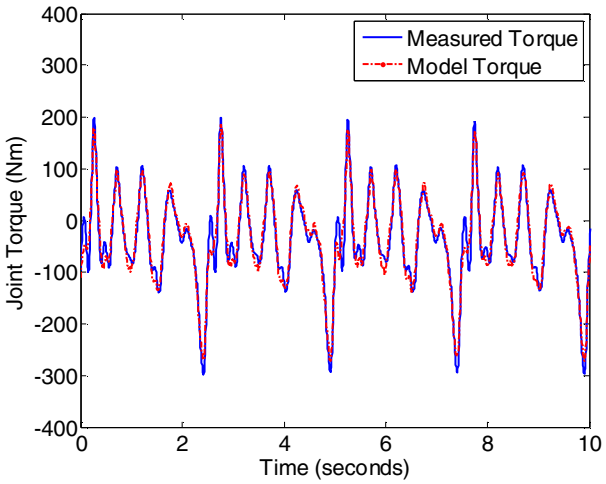

Fig. 5 Motor Torque for Joint 2

Joint stiffnesses were determined from a linear regression of the joint deflection and corresponding reconstructed stiffness torque (Fig. 6). The estimated parameters ranged from 4.78×10^2 in joint 6 to 1.19×10^4 in joint 2 (Table I). The r^2 correlation coefficients for joints 1 through 6 were equal to [0.66, 0.64, 0.54, 0.84, 0.71, 0.55].

VI. Conclusions

A rigid-link flexible-joint model accurately represents the dynamic behavior of the Mitsubishi PA10-6CE. The largest RMS residuals occurred in the identification of joint 2, corresponding to less than 8% of the amplitude of motor torque. The remaining joints all have residuals proportional to their motor torque. CV percentages for all friction and inertial parameter estimates were below 12%. Mass center estimates had slightly higher CV percentages because of smaller magnitudes. The resulting joint stiffnesses are similar in magnitude to estimates obtained through static calibration [16].

Principal sources of error in the identification process are measurement and synchronization errors in the joint angle, input torque, and motion capture measurements. The remaining differences between the predicted and actual motor torque result from unmodeled dynamics. An example is position-dependent friction arising from manufacturing errors and misalignment of the harmonic drive components during assembly [17]. There may also have been a disturbance torque acting on the actuated link from adjacent links. An electro-magnetic brake will fix motor position, but the harmonic drive may flex due to adjacent link motion. A better identification might be possible with a complete n-link identification method. Furthermore, errors in the stiffness calculation will arise from nonlinearities in the harmonic drive transmission, such as soft wind-up and hysteresis which occur in regions of low applied torque [18].

The advantage of separating the identification process into two steps is clear. The condition number of the reformulated regressor matrix is smaller, leading to improved robustness to noise in the regressor matrix and torque measurements. More importantly, one has more insight and flexibility in determining the torsional spring model from the computed

TABLE I
Parameter Identification Results

Joint	Statistic	I ($kg\ m^2$)	c (Nm)	v ($Nm\ s$)	mgl_x (Nm)	mgl_y (Nm)	b ($Nm\ s$)	J ($kg\ m^2$)	k (Nm/rad)	$error$ (Nm)
1	Mean	1.13	9.08	9.88	1.52	2.08	10.05	1.06	5.98×10^3	2.48
	CV (%)	0.64	1.75	1.87	1.78	3.59	1.75	0.64	3.86	2.38
2	Mean	6.15	9.28	18.38	111.64	-7.80	23.28	12.57	1.19×10^4	19.33
	CV (%)	9.62	11.07	6.82	4.47	16.89	6.15	5.33	4.74	3.72
3	Mean	2.27	5.81	5.79	8.33	8.56	6.35	2.48	4.60×10^3	6.55
	CV (%)	0.50	0.67	0.87	0.93	0.64	0.58	0.18	2.90	1.12
4	Mean	0.03	1.48	1.45	< 0.01	0.18	1.46	0.03	7.09×10^2	0.56
	CV (%)	0.68	6.50	7.02	n/a*	33.81	7.33	3.72	5.05	8.83
5	Mean	0.16	1.84	1.75	0.26	0.63	1.78	0.16	7.72×10^2	1.37
	CV (%)	0.68	4.96	5.13	1.34	8.01	5.39	0.44	5.17	3.76
6	Mean	0.08	0.87	0.92	0.10	< 0.01	0.96	0.07	4.78×10^2	0.33
	CV (%)	0.43	0.95	0.70	6.12	n/a*	0.83	0.36	0.74	1.21

* not applicable for parameter estimates which equal zero.

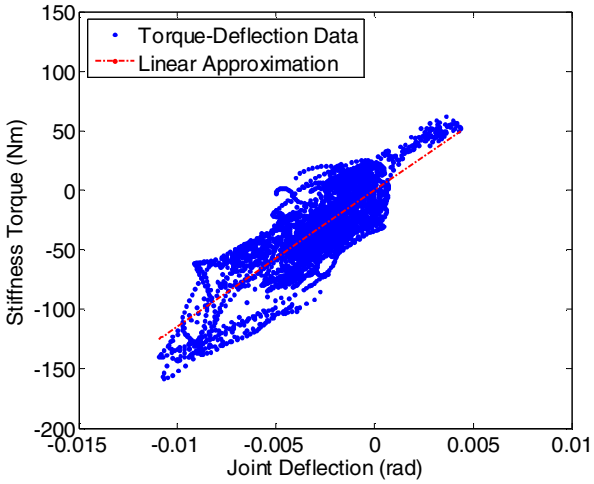

Fig. 6 Joint Deflection for Joint 2

stiffness torques. It presents no additional complexity to fit a cubic spring model to the measured joint deflection and stiffness torque. However, a cubic element in the regressor matrix would damage the identification process because of its much smaller size compared to other regressor elements. Furthermore, one can represent the torsional spring stiffness with non linear-parameterizable phenomenon, such as hysteresis [19]. This effect is common in harmonic drives, and it is unidentifiable through traditional linear least-squares identification.

Using motion capture for link position measurement is an important element of the identification method. Several researchers, e.g. Khalil [20], have used motion capture as part of their identification strategy, but the present study is an improvement upon previous work. Recently, there have been significant improvements in the accuracy, robustness, real-time measurement capabilities, and sampling frequency of motion capture systems. These improvements and lower costs make motion capture systems an increasingly attractive option for identification and real-time control of robotic systems.

Future efforts will be directed toward using a rigid-link flexible-joint model in model-based control algorithms [21]. The principal challenge in implementing such a controller is the measurement of link position in real-time. In this case, a nonlinear observer integrating joint resolver and motion capture information will be used to estimate link position in real-time.

ACKNOWLEDGMENT

The authors thank J.D. Yamokoski for help in programming and operation of the PA10-6CE and Jessica Allen for help in the friction identification.

REFERENCES

[1] M. Ostring, “Identification, diagnosis, and control of a flexible robot arm,” Linkoping Studies in Science and Technology, Thesis No. 948, Linkoping, Sweden, 2002.

[2] Yangmin Li, Xiaoping Liu, Zhaoyang Peng, and Yugang Liu, “The identification of joint parameters for modular robots using fuzzy theory and a genetic algorithm,” *Robotica*, vol. 20, pp. 509-517, 2002.

[3] H.D. Taghirad, P.R. Belanger, and A. Helmy, "An experimental study on harmonic drives", Technical Report submitted to International Submarine Engineering Ltd., McGill University Center for Intelligent Machines, 1996.

[4] A. Albu-Schaffer, and G. Hirzinger, “Parameter identification and passivity based joint control for a 7 DOF torque controller lightweight robot,” *Proc. of 2001 IEEE Int. Conf. on Robot. and Autom.*, pp 2852-2858, May 2001.

[5] B. Armstrong, “On finding exciting trajectories for identification experiments involving systems with nonlinear dynamics”, *Int. J. Robotics Res.*, vol. 8, pp. 28–48, 1989.

[6] J. Swevers, J. Ganseman, and H. Van Brussel, “Experimental robot identification using optimised periodic trajectories,” *Mechanical Systems and Signal Processing*, vol. 10, no. 5, pp. 561-577, 1996.

[7] G. Calafiore, M. Indri, and B. Bona, “Robot dynamic calibration: optimal excitation trajectories and experimental parameter estimation”, *Journal of Robotic Systems*, vol. 18, no. 2, pp. 55–68, 2001.

[8] M.T. Pham, M. Gautier, and P. Poignet, “Identification of joint stiffness with bandpass filtering,” *Proc. of the 2001 IEEE Int. Conf. on Robot. and Autom.*, pp. 2867-2872, May, 2001.

[9] M. Spong, “Modeling and control of elastic joint robots,” *Journal of Dyn. Syst., Meas. and Cont.*, vol. 109, pp. 310-319, 1987.

[10] S.S.H.U. Gamage, J. Lasenby, “New least squares solutions for estimating the average centre of rotation and the axis of rotation,” *Journal of Biomechanics*, vol. 35, pp. 87–93, 2002.

[11] K. Halvorsen, “Bias compensated least squares estimate of the center of rotation,” *Journal of Biomechanics*, vol. 36, pp. 999–1008, 2003.

[12] J.A. Reinbolt, J.F. Schutte, B.J. Fregly, R.T. Haftka, A.D. George, and K.H. Mitchell, "Determination of patient-specific multi-joint kinematic models through two-level optimization," *Journal of Biomechics,* vol. 38, pp. 621–626, 2004.

[13] “The Orocos Project,” Nov. 2002. [Online]. Available: http://www.orocos.org/.

[14] “Orca: Components for Robotics,” June 2002. [Online]. Available: http://orca-robotics.sourceforge.net/.

[15] Variable Resolution, Monolithic Resolver-to-Digital Converters, Analog Devices, Inc., Norwood, MA, 1998.

[16] C. Lightcap, S. Hamner, T. Schmitz, and S. Banks, “Improved positioning accuracy of the PA10-6CE robot with geometric and flexibility calibration,” *IEEE Trans. on Robotics*, submitted for publication, Jan. 2007.

[17] T.D. Tuttle, "Understanding and modeling the behavior of a harmonic drive gear transmission", Technical Report 1365, MIT Artificial Intelligence Laboratory, 1992.

[18] N. Kircanski, and A.A. Goldenberg, "An experimental study of nonlinear stiffness, hysteresis, and friction effects in robot joints with harmonic drives and torque sensors", *Int. J. Robot. Res.*, vol. 16, no. 2, pp. 214-239, 1997.

[19] R. Dhaouadi, F.H. Ghorbel, S.G. Prasanna, “A new dynamic model of hysteresis in harmonic drives,” *IEEE Trans. on Industrial Electronics*, vol. 50, no. 6, 2003.

[20] W. Khalil, and S. Besnard, "Geometric calibration of robots with flexible joints and links", *Journal of Intelligent and Robotic Systems*., vol. 34, 2002, pp. 357-379.

[21] W.E. Dixon, E. Zergeroglu, D.M. Dawson, and M.W. Hannan, "Global adaptive partial state feedback tracking control of rigid-link flexible-joint robots", *Robotica*, vol. 18, no. 3, pp. 325–336, 2000.